Title

The RodA Hydrophobin on Aspergillus fumigatus Spores Masks Dectin-1– and Dectin-2–Dependent Responses and Enhances Fungal Survival In Vivo

Journal

The Journal of Immunology, 191(5)

ISSN

0022-1767

Authors

de Jesus Carrion, Steven
Leal, Sixto M
Ghannoum, Mahmoud A
et al.

Publication Date

2013-09-01

DOI

10.4049/jimmunol.1300748

Peer reviewed

Published in final edited form as:
J Immunol. 2013 September 1; 191(5): 2581–2588. doi:10.4049/jimmunol.1300748.

The RodA hydrophobin on *Aspergillus fumigatus* spores masks Dectin-1 and Dectin-2 dependent responses and enhances fungal survival *in vivo*

Steven de Jesus Carrion[1], **Sixto M. Leal Jr.**[1], **Mahmoud A. Ghannoum**[2], and **Eric Pearlman**[1,*]

[1]Department of Ophthalmology and Visual Sciences, Case Western Reserve University, Cleveland, Ohio

[2]Center for Medical Mycology, Case Western Reserve University, Cleveland, Ohio

Abstract

Aspergillus and *Fusarium* species are important causes of fungal infections worldwide. Airborne spores (conidia) of these filamentous fungi express a surface protein that confers hydrophobicity (hydrophobin), and which covers cell wall components that would otherwise induce a host immune cell response. Using a mutant *Aspergillus fumigatus* strain that does not express the RodA hydrophobin (Δ*rodA)*, and *Aspergillus* and *Fusarium* conidia from clinical isolates that were treated with hydrofluoric acid (HF, which removes the *A. fumigatus* RodA protein), we observed increased surface exposure of β1,3-glucan and α-mannose on *Aspergillus* and *Fusarium* conidia. We also found that Δ*rodA* and HF treated conidia stimulate significantly higher NF-κB p65 nuclear translocation and cytokine production by macrophages from C57BL/6, but not from Dectin-$1^{-/-}$ or Dectin-$2^{-/-}$ mice. Using a murine model of *A. fumigatus* corneal infection, we found that Δ*rodA* conidia exhibited increased cytokine production, neutrophil infiltration, and more rapid fungal clearance from C57BL/6 corneas compared with the parent G10 strain, which was dependent on Dectin-1 and Dectin-2. Together, these findings identify the hydrophobin RodA as a virulence factor that masks Dectin-1 and Dectin-2 recognition of conidia, resulting in impaired neutrophil recruitment to the cornea and increased fungal survival and clinical disease.

Introduction

Although *Aspergillus* spores (conidia) and those of other filamentous fungi are ubiquitous in the air we breathe and can reach high concentrations (>10^9 spores per cubic meter in some environments), they do not generally cause inflammatory disease following inhalation (1, 2). Fungal cell wall components such as β1,3-glucan and α-mannan have the potential to induce inflammation; however, conidia are coated by a hydrophobic “rodlet layer” composed of regularly arranged RodA hydrophobins, which are covalently bound to cell wall polysaccharides by glycosylphosphatidylinositol (GPI) anchor proteins (3, 4). A recent study showed that removal of *A. fumigatus* RodA by hydrofluoric acid, which cleaves the

*Corresponding author Eric Pearlman 10900 Euclid Ave Cleveland OH 44106 Tel: 216 368 1856 Fax: 216 368 3171 Eric.Pearlman@case.edu.

phosphodiester bonds attaching RodA to the cell wall, confers conidia recognition by human dendritic cells and murine alveolar macrophages (5). Also, mice infected with an *A. fumigatus* Δ*rodA* mutant caused increased lung inflammation compared with the parent strain (5). As *Aspergillus* and *Fusarium* species are also major causes of corneal infection and blindness worldwide (6), the current study examined the role of hydrophobins in a murine model of fungal keratitis (7, 8). We also identified cell wall components that are exposed in the absence of RodA, and the pathogen recognition molecules that are activated.

We show that β1,3-glucan and α-mannan are exposed on the cell wall of *Aspergillus* conidia in the absence of RodA, and that the c-type lectins Dectin-1 and Dectin-2 mediate the host response. Using a murine model of *Aspergillus* corneal infection, we also demonstrate that in the absence of RodA, *A. fumigatus* induces Dectin-1 and Dectin-2 dependent neutrophil recruitment to the corneal stroma and enhanced fungal killing. Together, these data represent a novel fungal adaptation to evade early recognition by Dectin-1 and Dectin-2, enabling conidia to germinate and form hyphae prior to immune recognition, which thereby enhances fungal survival during infection.

Materials and Methods

Source of mice

All animals were treated in accordance with the guidelines provided in the Association for Research in Vision and Ophthalmology ARVO statement for the Use of Animals in Ophthalmic and Vision Research, and were approved by Case Western Reserve University IACUC. C57Bl/6 mice (5-12 week old) were purchased from The Jackson Laboratory (Bar Harbor, ME). Dectin-1 and Dectin-2 deficient mice were a kind gift from Yoichiro Iwakura (University of Tokyo, Japan).

Fungal strains, media, and growth conditions

Aspergillus strains used in this study were cultured in Vogel's minimal media (VMM) w/wo 4% agar +/− supplementation with 10mM uracil and 5mM uridine at 37°C/5%CO_2 unless stated otherwise. The *A. fumigatus* parent (G10) and mutant (Δ*rodA*) strains were provided by Jean Paul-Latge (Institut Pasteur, Paris, France) *A. fumigatus* Af-BP strain is a clinical isolate from a patient treated at Bascom Palmer Eye Institute (Miami, FL), provided by Dr. Darlene Miller. The *F. oxysporum* 8996 strain is a clinical isolate from a patient treated at the Cleveland Clinic Institute (Cleveland, Ohio) (8). The *A. flavus* TN-302 strain is a clinical isolate obtained from the Aravind Eye Hospital-Madurai, Tamil Nadu, India. *F. solani* B6970 was from a contact lens keratitis patient and obtained from the Centers for Disease Control.

RodA protein extraction method

The rodlet layer was extracted from the cell wall by incubating dry spores with 4% hydrofluoric acid (HF) for 72h at 4°C. The content was centrifuged (10,000rpm, 10min) and supernatant was discarded. Samples were fixed with 4% paraformaldehyde for 30min and washed 3X with sterile PBS.

Detection of surface β1,3-glucan and α-mannose

Aspergillus strains were cultured for 3 days in VMM+4% agar and *Fusarium* strains were cultured in SDA media. Pure conidial suspensions were prepared from the 3-day culture and fixed in 4% PFA as described before. Conidia were centrifuged (10,000rpm, 5min) and blocked with 1.5% normal rabbit serum in PBS for 1h, then incubated with a Dectin-1 Fc fusion protein (9)), which was a gift from Dr Chad Steele, University of Alabama at Birmingham Conidia were then washed 3x with PBS and incubated with FITC-conjugated goat-anti-mouse IgG (Invitrogen) diluted to 1mg/ ml in PBS for 1h at 37°C.

Murine model of corneal infection

A. fumigatus strains were cultured in VMM agar in 25cm^2 tissue culture flasks. Dormant conidiawere disrupted with a bacterial L-loop and harvested in 5ml PBS. Pure conidial suspensions were obtained by passing the culture suspension through PBS-soaked sterile gauges placed at the tip of a 10ml syringe. Conidia were quantified using a hemacytometer and a stock was made at a final concentration of 2.5×10^4conidia/μl in PBS. Mice were anaesthetized by intraperitoneal (IP) injection of 0.6% Tribromoethanol, 1.2% tert-butyl alcohol, and PBS. Corneal epithelium was abraded with a 30 gauge needle. Through the abrasion was inserted a 33-gauge Hamilton needle and a 2 μl injection containing 5×10^4 conidia (Optimal inoculum to study the disease was determined by preliminary studies; data not shown) was released into the corneal stroma. Mice were examined daily under a stereomicroscope for corneal opacification, ulceration, and perforation. At set time points, animals were euthanized by CO_2 asphyxiation, and eyes were either placed in 10% formalin and embedded in paraffin and sectioned at 5 micron intervals, or excised and placed in 1 ml of sterile saline and homogenized for quantitative culture. All animals were bred under specific pathogen-free conditions and maintained according to institutional guidelines.

Imaging corneal opacity

Mice were sacrificed by CO_2 asphyxiation and positioned in a three-point stereotactic mouse restrainer. Corneal opacity (Brightfield) was visualized in the intact cornea using a high resolution stereo fluorescence MZFLIII microscope (Leica Microsystems) and Spot RT Slider KE camera (Diagnostics Instruments). All images were captured using SpotCam software (RT Slider KE; Diagnostics Instruments).

Quantification of colony forming units (CFUs)

For assessment of fungal viability, whole eyes were homogenized under sterile conditions in 1 ml PBS, using the Mixer Mill MM300 (Retsch, Qiagen, Valencia, CA) at 33 Hz for 4 min. Subsequently, serial log dilutions were performed and plated onto Sabouraud dextrose agar plates (Becton Dickenson). Following incubation for 24h at 37° C, the number of CFUs was determined by direct counting.

Identification of fungi and inflammatory cell recruitment

Eyes were enucleated and fixed in 10% formalin in PBS (Fisher) for 24h. Tissues were then dehydrated in graded ethanol concentrations at room temperature (65% 1x, 80% 2x, 95% 1x, 100% 3x; 1 h for each change of solution), followed by three 1h changes of xylene, and 4

changes of paraffin at 60oC under 15mm Hg vacuum to remove air bubbles. Five mm sections from the center of the cornea (as determined by noncontiguous iris morphology) were cut and stained with Periodic-Acid Schiff (PASH) for identification of fungi and inflammatory cell recruitment.

Immunohistochemistry

To detect neutrophils during live corneal infection, 5 micron paraffin sections were deparaffinized. Slides were blocked with 1.5% normal rabbit serum in PBS for 1h, then incubated with monoclonal rat-anti-mouse neutrophil IgG (NIMP-R14, AbCam, Cambridge, MA), for 1h at 37°C. The slides were then washed 3x in PBS plus 0.05% Tween20 (PBS-T; Sigma) and incubated with alexafluor-488 tagged rabbit-anti-rat IgG (Invitrogen) for 1h at 37°C. The slides were washed 3x in PBS-T and imaged by fluorescence microscopy (magnification, 40x).

Isolation of peritoneal and bone marrow derived macrophages (BMM)

For peritoneal macrophages, 1.5mL of 4% thioglycolate was injected into the peritoneal cavity of naïve mice. Three days later, mice underwent euthanasia by CO_2 asphyxiation and macrophages were isolated from the peritoneal cavity in sterile PBS using a 10mL syringe (BD syringes). Red blood cells were lysed using 1X RBC lysis buffer (eBioscience) and washed in sterile PBS. Cells were then counted and harvested.

For bone marrow macrophage isolation, mice were euthanized by CO_2 asphyxation and femurs and tibias were removed, cleaned, and centrifuged at 6000xg for 45s at 4°C. Any contaminating red blood cells were lysed in 5 ml RBC Lysis Buffer (eBioscience), and remaining bone marrow cells were cultured in bacteriologic grade petri dishes in 6 ml Macrophage Growth Medium (MGM:DMEM w/L- Glutamine, Na-Pyruvate, HEPES,10% FBS, P/S, 30% L929 cell conditioned medium). On day 5, and every 2 days thereafter, the cell supernatant was aspirated, and fresh MGM media was added. Adherent cells were harvested between 7–14 days of culture, and counted.

Detection of NFκB nuclear translocation and cell-associated conidia in bone marrow derived macrophages (BMDM)

Adherent cells were harvested between 7–14 days of culture. 2.5×10^4 cells were cultured onto sterile 18mm2 coverslips (Corning) in a 6 well-plate, and treated with LPS (100 ng/ml; positive control), G10, and Δ*rodA* conidia (MOI =100) for 15, 30 and 60 min. Following activation, BMM were fixed with 4% paraformaldehyde for 15 min at room temperature, permeabilized using 0.1% Triton X-100 in PBS for 1 min at RT, and incubated with rabbit anti-mouse p65 (1:100; eBioscience Ltd) in PBS containing 10% goat serum for 1h at RT. Coverslips were washed 2x with PBS and cells were incubated with Alexa Fluor 488-labeled goat anti-rabbit IgG antibody (Molecular Probes Inc.) in PBS at RT for 1h and washed 2x with PBS. The cells were mounted on glass slides using Vectashield mounting medium with DAPI (Vector Laboratories, UK), and examined by fluorescence microscopy.

For cell association studies, bone marrow macrophages incubated with naïve or hydrofluoric acid (HF) treated conidia were washed and fixed in 4% paraformaldehyde as described

above, then incubated 5 min with Calcofluor white (Sigma) at a 1:1 ratio with 10% KOH. After washing 2x with PBS, cells were examined by DIC and fluorescence microscopy, and associated conidia per 100 cells, and the percent cells with associated conidia was determined after direct examination of at least 50 cells per coverslip. Two coverslips were examined, and the mean and SD were calculated.

Cytokine Assays

Peritoneal macrophages were incubated with naïve, HF treated, and Δ*rodA* dormant conidia for 6h and cell culture supernatants were obtained. LPS (10ng/ml, Invitrogen) and Curdlan (100μg/ml, Invivogen) were used as controls for stimulations. In Syk inhibition experiments, Piceatannol (50μM, Sigma) was added 30min prior to stimulation. Half-well cytokine assays were performed using Duoset ELISA kits (R & D Systems) according to the manufacturer's directions.

Image Analysis

To quantify the NIMP stained histological sections, we obtained the images in 12 bits on a Leica DMI 6000 B inverted microscope using a 40x objective connected to a Retiga EXI camera (Q-imaging Vancouver British Columbia). Analysis was performed using Metamorph Imaging Software (Molecular Devices Downington, PA). Images were stitched together to create an entire cornea. The area of the cornea was delineated and recorded. Next the image was thresholded to recognize the NIMP staining. This resulting NIMP area within the cornea was recorded and utilized to plot a graph.

To quantify corneal opacity, brightfield images of mouse corneas were analyzed using Metamorph software (Molecular Devices) as described (6, 19). Briefly, a constant circular region encompassing the cornea was defined, and the pixel intensity within this region summed to yield a numerical value which corresponds to the total amount of light reflected from the cornea (i.e. opacity). Images were taken in a Spot RT Slider KE camera using Spot Advanced Software under the same magnification, exposure, and gamma parameters.

Statistical Analysis

Statistical analysis was performed for each experiment using an unpaired t test (Prism, GraphPad Software). A P value of <0.05 was considered significant.

Results

RodA protein masks surface β1,3-glucan and α-mannose in Aspergillus and Fusarium conidia and masks cytokine production by macrophages

Fusarium species, which cause systemic disease and corneal infections (10-12), also express hydrophobins (13). Therefore, we treated *Aspergillus* and *Fusarium* conidia from clinical isolates with hydrofluoric acid (HF), which unmasks the RodA hydrophobin from *A. fumigatus* as previously shown (5). We also examined the *A. fumigatus* RodA mutant and the parent G10 strain as described (5).

Using a Dectin-1 Fc fusion protein to detect β1,3-glucan (9), we found increased binding to Δ*rodA* compared with G10 conidia **(Figure 1A)**. Similarly, there was increased binding to HF treated *Aspergillus* and *Fusarium* conidia compared with untreated. Since α-mannose is also abundant in the fungal cell wall, we used the lectin Concavalin A (ConA) to detect this sugar on the cell surface. **Figure 1B** shows higher α-mannose staining on Δ*rodA* conidia compared with the G10 strain, and increased binding on HF treated *Aspergillus* and *Fusarium* clinical isolates compared with untreated conidia. We further confirmed this data by detecting β1,3-glucan and α-mannose on the surface of Δ*rodA* conidia by confocal microscopy (Figure S1).

As the RodA protein confers resistance to phagocytosis (14), we examined cytokine production in macrophages incubated with Δ*rodA* and HF treated conidia. **Figure 1C** shows significantly higher CXCL1, CXCL2, and TNF-α production by macrophages incubated with *Aspergillus* Δ*rodA* and *Fusarium* HF treated conidia compared with the G10 strain or untreated *Fusarium* conidia.

These data indicate that the hydrophobic RodA protein masks surface β1,3-glucan and α-mannose in *Aspergillus* conidia, and that HF treatment removes molecules that share a similar function as RodA on *Fusarium* conidia.

Dectin-1 and Dectin-2 are required for conidia-induced macrophage NFkB translocation and cytokine production in the absence of RodA

To determine if the increased cytokine production in the absence of RodA protein is related to macrophage binding or uptake of conidia, we incubated C57BL/6, Dectin-1$^{-/-}$ and Dectin-2$^{-/-}$ bone marrow macrophages with Δ*rodA* conidia at a multiplicity of infection (MOI) of 100, and the number of conidia bound or internalized by macrophages was imaged by DIC microscopy and quantified by direct counting. As shown in **Figures 2A-B**, the average number of associated Δ*rodA* conidia per macrophage was significantly higher than G10 conidia.

To assess the role of c-type lectins in conidia-induced macrophage activation in the absence of RodA, Dectin-1$^{-/-}$ and Dectin-2$^{-/-}$ bone marrow macrophages were incubated 1h with Δ*rodA* conidia, and nuclear translocation of the p65 subunit of NFκB was detected by immunofluorescence and DAPI nuclear stain. As shown in **Figures 2C-D**, following LPS incubation, p65 was detected in the nucleus of C57Bl/6, Dectin-1$^{-/-}$ and Dectin-2$^{-/-}$ macrophages. In contrast, nuclear localization of p65 was detected in C57Bl/6, but not Dectin-1$^{-/-}$ or Dectin-2$^{-/-}$macrophages incubated with Δ*rodA* conidia, whereas the G10 strain failed to induce p65 translocation in C57Bl/6, Dectin-1$^{-/-}$ or Dectin-2$^{-/-}$ macrophages.

To determine if Dectin-1 and Dectin-2-dependent p65 translocation also affects cytokine production, macrophages were incubated for 6h with Δ*rodA* and HF treated *Fusarium* conidia, and cytokine production was measured by ELISA. **Figure 2E** shows significantly less CXCL1, CXCL2, and TNF-α production by Dectin-1$^{-/-}$ compared with C57Bl/6 macrophages stimulated with Δ*rodA*, whereas Dectin-2$^{-/-}$ macrophages produced significantly less CXCL2 and TNF-α (although CXCL1 production was lower, the

difference was not statistically significant). Consistent with the absence of p65 translocation, cytokines were not detected following incubation with the G10 parental strain. These results indicate that the *Aspergillus* RodA protein and HF sensitive *Fusarium* molecules mask Dectin-1 and Dectin-2 recognition of conidia by macrophages, resulting in impaired cytokine production.

Cytokine production induced by ΔrodA and HF conidia is dependent on spleen tyrosine kinase

Spleen tyrosine kinase (Syk) mediates Dectin-1 and Dectin-2 signaling in macrophages and dendritic cells (15). Syk contains two SH-2 domains that allow it to bind phosphorylated tyrosines in the ITAM-like motif of Dectin-1 and in the ITAM motif of the Fc receptor that associates with Dectin-2. Syk kinase activity then mediates downstream signaling and activation of the nuclear factor kappa-light-chain-enhancer of activated B cells (NFκB) to activate transcription of target genes (15-18).

To examine the role of Syk in conidia-induced cytokine production, C57Bl/6 bone marrow macrophages were incubated with LPS (which signals through TLR4), curdlan, Δ*rodA*, and *Fusarium* HF treated conidia in the presence of the Syk inhibitor Piceatannol. As shown in **Figure 3,** LPS-induced cytokine production was not inhibited, consistent with the TLR4 pathway being mostly Syk-independent (although internalized TLR4 activates Syk (19)). In contrast curdlan-induced production of CXCL1, CXCL2, and TNF-α was significantly lower in the presence of Piceatannol. Cytokine production induced by Δ*rodA* and *Fusarium* HF treated conidia was also significantly lower in the presence of Piceatannol, indicating that the Syk-dependent pathway is essential for the increase in cytokine production. As before, cytokines were not detected following stimulation with G10 or HF untreated conidia.

RodA protein enhances fungal survival in vivo

While Δ*rodA* mutants were shown to induce more lung inflammation than G10 (20), the role of RodA in fungal survival and clinical disease has yet to be determined. To examine the role of RodA, we used a murine model of *A. fumigatus* corneal infection in which conidia are injected directly into the corneal stroma of immunocompetent, C57BL/6 mice. Conidia germinate and spread throughout the cornea, stimulating a pronounced neutrophil infiltrate and corneal opacification (7, 21). C57BL/6 mice were then infected with G10 or Δ*rodA* conidia, and disease progression, neutrophil infiltration, and fungal viability were assessed.

As shown in **Figure 4A-C,** corneas infected with the G10 parent strain developed progressively increasing corneal opacification over 72h (quantification of corneal opacity is described in **Figure S2)**, which is consistent with our earlier findings using other *A. fumigatus* strains (7, 21), and in our model of *Fusarium* keratitis (8). In contrast, corneas infected with the Δ*rodA* mutant exhibited significantly higher percent and total corneal opacity at 24h, but had significantly less disease at 48h and 72h. Consistent with the 24h opacification data, we found that neutrophil and macrophage infiltration into the corneal stroma was significantly elevated in mice infected with the Δ*rodA* mutant at 24h post-infection compared with the G10 parent strain (**Figure 4D, E**). Further, there was significantly less colony forming units (CFUs) in the Δ*rodA* compared with G10 infected

corneas at each time point. Four of the five mice given the Δ*rodA* strain completely cleared the infection by 96h (**Figure 4F**).

We conclude from these data that the Δ*rodA* strain induced more rapid cellular infiltration and fungal killing than the parent strain, with the cellular infiltration causing more corneal opacity at 24h. Conversely, the host response to the parent G10 strain is delayed due to expression of RodA, causing a more protracted infiltrate and prolonged corneal opacity.

These findings clearly demonstrate that the RodA hydrophobin enhances fungal survival *in vivo* resulting in prolonged and exacerbated corneal disease.

ΔrodA induces Dectin-1 and Dectin-2 dependent increased cytokine production and neutrophil recruitment to the cornea

Results of our previous studies on *Aspergillus* and *Fusarium* keratitis suggested a sequence of events in which Dectin-1 dependent cytokine production by resident macrophages induces neutrophil recruitment to the cornea stroma and mediates hyphal killing (22). To examine if the enhanced clearance of Δ*rodA* conidia from infected corneas is due to a more rapid or robust cytokine response and neutrophil infiltration, and to determine the role of Dectin-1 and Dectin-2, we infected Dectin-$1^{-/-}$ and Dectin-$2^{-/-}$ mice with G10 or Δ*rodA* conidia. After 6h, cytokine production and neutrophil infiltration were quantified.

Figure 5A shows that at 6h post infection, there were significantly higher CXCL1, CXCL2, and IL-6 levels in C57BL/6 corneas infected with Δ*rodA* compared to the G10 strain. Further, whereas there were no significant differences in cytokine production among Dectin-$1^{-/-}$, Dectin-$2^{-/-}$ and C57BL/6 corneas infected with the G10 strain, production of each cytokine was significantly lower in Δ*rodA* infected corneas of Dectin-$1^{-/-}$ and Dectin-$2^{-/-}$ compared with C57Bl/6 mice.

As normal corneas are avascular and have resident macrophages, but not neutrophils, we examined neutrophil infiltration using the Ly6G antibody NIMP-R14 to identify these cells in 5μm corneal sections. Consistent with the chemokine data, the amount of neutrophils in G10 infected Dectin-$1^{-/-}$ and Dectin-$2^{-/-}$ corneas at 6h post-infection was not significantly different from C57BL/6 corneas (**Figure 5B, C**). In contrast, Δ*rodA* infected C57BL/6 corneas had a significantly higher neutrophil infiltrate compared with the G10 strain, which was significantly lower in Dectin-$1^{-/-}$ and Dectin-$2^{-/-}$ corneas. These data indicate that the early cytokine production and neutrophil recruitment induced by Δ*rodA* conidia are dependent on Dectin-1 and Dectin-2.

Dectin-1 and Dectin-2 regulate corneal opacification and fungal killing following infection with ΔrodA conidia

To determine if there is a role for Dectin-1 and Dectin-2 in fungal clearance of Δ*rodA* and G10 from infected corneas, Dectin-$1^{-/-}$ and Dectin-$2^{-/-}$ mice were infected instrastromally with live conidia as before, and examined after 24h when there was a clear difference in CFU, cellular infiltration and corneal opacity (**Figure 5**).

Figure 6A shows that as in Figure 5, there were significantly less CFUs in Δ*rodA* compared with G10 infected corneas of C57Bl/6 mice at 24h post-infection, indicating more efficient killing of the Δ*rodA* strain. In contrast, CFU of Dectin-$1^{-/-}$ and Dectin-$2^{-/-}$ corneas infected with Δ*rodA* were significantly higher than C57Bl/6 mice, indicating an essential role for Dectin-1 and Dectin-2 in fungal killing. There was no significant difference in CFU between C57BL/6 Dectin-$1^{-/-}$ and Dectin-$2^{-/-}$ infected with G10 at this time point.

Conversely, **Figures 6B-D** show that corneal opacification in Δ*rodA* infected C57Bl/6 mice was significantly lower in Dectin-$1^{-/-}$ and Dectin-$2^{-/-}$ mice, indicating that these receptors also mediate corneal disease in the absence of RodA. Interestingly, the parent G10 strain, which based on our prior studies using related *A. fumigatus* strains would have germinated and partially exposed surface α-glucan 24h post infection (7), has significantly less corneal opacity in Dectin-$1^{-/-}$ compared with C57BL/6 corneas. Consistent with these findings and with the role for neutrophils in corneal opacification (21), there were also significantly less neutrophils in G10 and Δ*rodA* infected Dectin-$1^{-/-}$ and Dectin-$2^{-/-}$ corneas compared with C57BL/6 mice (**Figure 6E**). Furthermore, there was significantly more neutrophil infiltration in Δ*rodA* compared with G10 infected C57BL/6 corneas, consistent with increased corneal opacity.

Taken together, these data indicate that the RodA hydrophobin masks Dectin-1 and Dectin-2 recognition of exposed fungal cell wall β-glucan and α-mannose, impairing neutrophil recruitment to the cornea and facilitating fungal survival.

Discussion

The innate immune system recognizes microorganisms through a limited number of germline-encoded pathogen recognition receptors, which have the ability to trigger intracellular signaling pathways to eliminate infectious organisms in the body (23). In fungal infections, the C-type lectins are the largest and most diverse lectin family and comprise receptors that can bind to fungal glycan ligands in a calcium-dependent manner (24, 25). In the current study, we show that the *A. fumigatus* RodA hydrophobin masks surface β1,3-glucan and α-mannose in dormant *A. fumigatus* and *A. flavus* conidia in strains isolated from patients with corneal ulcers. This hydrophobic protein blocks Dectin-1 and Dectin-2 recognition of conidia, thereby evading Syk-dependent cytokine production by macrophages in addition to phagocytosis. *In vivo*, we demonstrate that during corneal infection with *A. fumigatus*, blockade of Dectin-1 and Dectin-2 signaling leads to decreased neutrophil infiltration and enhanced survival in the cornea. Consistent with our findings using the *A. fumigatus* Δ*rodA* mutant, we show that HF treated *Fusarium* conidia results in exposure of surface β1,3-glucan and α-mannose, which are then recognized by Dectin-1 and Dectin-2 on macrophages and result in cytokine production. This indicates a novel role for the RodA protein in promoting fungal survival during *A. fumigatus* infection, and implies that other pathogenic filamentous fungi that express RodA or other molecules have a similar role in evading host immune responses.

Our findings are consistent with the elevated macrophage phagocytosis of *A. fumigatus* LaeA mutants (Δ*laeA*), which have lower RodA expression than the parent strain (26). Our

data also extend our understanding of the role of the rodA protein described by Latge et al in a recent study. These investigators showed that the ΔrodA mutant induced increased IL-6 and TNF-α production by macrophages , and more severe pulmonary inflammation in mice infected with *A. fumigatus* Δ*rodA* compared with the G10 parent strain (20). We confirmed these observations using a model of corneal infection, and increased our understanding of the mechanism by which hydrophobins prevent potentially damaging host cell responses to common airborne spores. Our *in vitro* and *in vivo* findings indicate that the RodA hydrophobin impairs macrophage recognition of spores by Dectin-1 and Dectin-2, which would otherwise induce elevated cytokine production by recognition of β1,3-glucan and α-mannose, in addition to increased phagocytosis. By blocking macrophage production of pro-inflammatory and chemotactic cytokines, recruitment of neutrophils to the site of infection is impaired, resulting in increased fungal growth. Masking of immunogenic cell wall components appears to be a broad strategy of fungal survival during infection as dormant yeasts such as *Candida albicans* and *Histoplasma capsulatum* do not expose β1,3-glucan on the surface until they form bud scars during the process of germination (27-29).

Although there is a clear role for Dectin-1 in recognizing β1,3-glucan and mediating the host response to germinating *A. fumigatus* (30, 31), less is known about the role of Dectin-2 during fungal infection. Our results showing a role for Dectin-1 and Dectin-2 in protection against infection with *A.fumigatus* Δ*rodA* are in agreement with the protective role of Dectin-2 in controlling *C. albicans* infection by inducing IL-23 production by dendritic cells generating a protective Th17 response (32). Consistent with this report, Dectin-2 activates the c-Rel subunit of NF-κB in human dendritic cells, which selectively induces IL-23 and IL-1β gene expression, and which is distinct from Dectin-1-mediated activation of all NF-κB subunits (33). In contrast, we found that Dectin-1 and Dectin-2 are the main receptors required for translocation of the p65 subunit of NF-κB to the nucleus, although we have yet to examine other subunits or the direct effect of p65 on cytokine gene expression. Further, blockade of Syk by Piceatannol did not exhibit an additive effect in cytokine production, suggesting that Syk-independent pathways downstream of Dectin-1 and Dectin-2 could also be contributing to the inflammatory response.

In the current study, we found that RodA protein enhances fungal viability and prevents Dectin-1 and Dectin-2 mediated recognition of conidia *in vivo*. These results suggest that opsonization of RodA protein with antibodies could potentiate phagocytosis and improve the outcome of infection. Also, since RodA protein is degraded at the site of germination, antibodies to RodA could potentially activate Fc receptors on macrophages and neutrophils to induce production of reactive oxygen species, which we found are essential for killing fungal hyphae (21).

In conclusion, the more rapid fungal killing of the Δ*rodA* strain in infected corneas indicates that this protein functions as a virulence factor that mediates fungal survival *in vivo* by masking Dectin-1 and Dectin-2 recognition by resident tissue macrophages. Impaired macrophage cytokine production and neutrophil recruitment to the site of infection allows time for spores to germinate and invade the tissue before an effective host response can develop. Therefore, future studies of the molecular pathways underlying hydrophobin formation and degradation, in addition to an increased understanding of the role of the host

response may identify potential therapeutic targets that could abrogate the consequences of infection with these pathogenic fungi.

Supplementary Material

Refer to Web version on PubMed Central for supplementary material.

Acknowledgments

The authors greatly appreciate the outstanding technical assistance of the Visual Sciences Research Center core facilities, especially Scott Howell, Catherine Doller and Dawn Smith.

This work was supported by NIH grants RO1 EY018612 (EP), P30 EY011373 (EP), and by the Research to Prevent Blindness Foundation and the Ohio Lions Eye Research Foundation.

References

1. Oliveira M, Ribeiro H, Delgado JL, Abreu I. The effects of meteorological factors on airborne fungal spore concentration in two areas differing in urbanisation level. Int J Biometeorol. 2009; 53:61–73. [PubMed: 19048306]
2. Mahieu LM, De Dooy JJ, Van Laer FA, Jansens H, Ieven MM. A prospective study on factors influencing aspergillus spore load in the air during renovation works in a neonatal intensive care unit. J Hosp Infect. 2000; 45:191–197. [PubMed: 10896797]
3. Latge JP. Tasting the fungal cell wall. Cell Microbiol. 2010; 12:863–872. [PubMed: 20482553]
4. Linder MB, Szilvay GR, Nakari-Setala T, Penttila ME. Hydrophobins: the protein-amphiphiles of filamentous fungi. Fems Microbiology Reviews. 2005; 29:877–896. [PubMed: 16219510]
5. Aimanianda V, Bayry J, Bozza S, Kniemeyer O, Perruccio K, Elluru SR, Clavaud C, Paris S, Brakhage AA, Kaveri SV, Romani L, Latge JP. Surface hydrophobin prevents immune recognition of airborne fungal spores. Nature. 2009; 460:1117–1121. [PubMed: 19713928]
6. Srinivasan M. Fungal keratitis. Curr Opin Ophthalmol. 2004; 15:321–327. [PubMed: 15232472]
7. Leal SM, Cowden S, Hsia YC, Ghannoum MA, Momany M, Pearlman E. Distinct Roles for Dectin-1 and TLR4 in the Pathogenesis of Aspergillus fumigatus Keratitis. Plos Pathogens. 2010; 6
8. Tarabishy AB, Aldabagh B, Sun Y, Imamura Y, Mukherjee PK, Lass JH, Ghannoum MA, Pearlman E. MyD88 regulation of Fusarium keratitis is dependent on TLR4 and IL-1R1 but not TLR2. Journal of Immunology. 2008; 181:593–600.
9. Mattila PE, Metz AE, Rapaka RR, Bauer LD, Steele C. Dectin-1 Fc targeting of aspergillus fumigatus beta-glucans augments innate defense against invasive pulmonary aspergillosis. Antimicrob Agents Chemother. 2008; 52:1171–1172. [PubMed: 18086835]
10. Chang DC, Grant GB, O'Donnell K, Wannemuehler KA, Noble-Wang J, Rao CY, Jacobson LM, Crowell CS, Sneed RS, Lewis FMT, Schaffzin JK, Kainer MA, Genese CA, Alfonso EC, Jones DB, Srinivasan A, Fridkin SK, Park BJ. Multistate outbreak of Fusarium keratitis associated with use of a contact lens solution. Jama-Journal of the American Medical Association. 2006; 296:953–963.
11. Dignani MC, Anaissie E. Human fusariosis. Clin Microbiol Infect 10 Suppl. 2004; 1:67–75.
12. Thomas PA. Fungal infections of the cornea. Eye (Lond). 2003; 17:852–862. [PubMed: 14631389]
13. Fuchs U, Czymmek KJ, Sweigard JA. Five hydrophobin genes in Fusarium verticillioides include two required for microconidial chain formation. Fungal Genet Biol. 2004; 41:852–864. [PubMed: 15288021]
14. Latge JP. The pathobiology of Aspergillus fumigatus. Trends Microbiol. 2001; 9:382–389. [PubMed: 11514221]
15. Mocsai A, Ruland J, Tybulewicz VL. The SYK tyrosine kinase: a crucial player in diverse biological functions. Nature Reviews Immunology. 2010; 10:387–402.

16. Rogers NC, Slack EC, Edwards AD, Nolte MA, Schulz O, Schweighoffer E, Williams DL, Gordon S, Tybulewicz VL, Brown GD, Reis e Sousa C. Sykdependent cytokine induction by Dectin-1 reveals a novel pattern recognition pathway for C type lectins. Immunity. 2005; 22:507–517. [PubMed: 15845454]
17. Kerrigan AM, Brown GD. Syk-coupled C-type lectin receptors that mediate cellular activation via single tyrosine based activation motifs. Immunol Rev. 2010; 234:335–352. [PubMed: 20193029]
18. Drummond RA, Saijo S, Iwakura Y, Brown GD. The role of Syk/CARD9 coupled C-type lectins in antifungal immunity. Eur J Immunol. 2011; 41:276–281. [PubMed: 21267996]
19. Zanoni I, Ostuni R, Marek LR, Barresi S, Barbalat R, Barton GM, Granucci F, Kagan JC. CD14 controls the LPS-induced endocytosis of Toll-like receptor 4. Cell. 2011; 147:868–880. [PubMed: 22078883]
20. Aimanianda V, Bayry J, Bozza S, Kniemeyer O, Perruccio K, Elluru SR, Clavaud C, Paris S, Brakhage AA, Kaveri SV, Romani L, Latge JP. Surface hydrophobin prevents immune recognition of airborne fungal spores. Nature. 2009; 460:1117–U1179. [PubMed: 19713928]
21. Leal SM Jr. Vareechon C, Cowden S, Cobb BA, Latge JP, Momany M, Pearlman E. Fungal antioxidant pathways promote survival against neutrophils during infection. Journal of Clinical Investigation. 2012; 122:2482–2498. [PubMed: 22706306]
22. Leal SM Jr. Pearlman E. The role of cytokines and pathogen recognition molecules in fungal keratitis - Insights from human disease and animal models. Cytokine. 2012; 58:107–111. [PubMed: 22280957]
23. Akira S, Uematsu S, Takeuchi O. Pathogen recognition and innate immunity. Cell. 2006; 124:783–801. [PubMed: 16497588]
24. Robinson MJ, Sancho D, Slack EC, LeibundGut-Landmann S, Sousa CRE. Myeloid C-type lectins in innate immunity. Nat Immunol. 2006; 7:1258–1265. [PubMed: 17110942]
25. Willment JA, Brown GD. C-type lectin receptors in antifungal immunity. Trends Microbiol. 2008; 16:27–32. [PubMed: 18160296]
26. Dagenais TR, Giles SS, Aimanianda V, Latge JP, Hull CM, Keller NP. Aspergillus fumigatus LaeA-mediated phagocytosis is associated with a decreased hydrophobin layer. Infect Immun. 2010; 78:823–829. [PubMed: 19917717]
27. Gantner BN, Simmons RM, Underhill DM. Dectin-1 mediates macrophage recognition of Candida albicans yeast but not filaments. Embo Journal. 2005; 24:1277–1286. [PubMed: 15729357]
28. Chamilos G, Ganguly D, Lande R, Gregorio J, Meller S, Goldman WE, Gilliet M, Kontoyiannis DP. Generation of IL-23 producing dendritic cells (DCs) by airborne fungi regulates fungal pathogenicity via the induction of T(H)-17 responses. PLoS One. 2010; 5:e12955. [PubMed: 20886035]
29. Rappleye CA, Eissenberg LG, Goldman WE. Histoplasma capsulatum alpha-(1,3)-glucan blocks innate immune recognition by the beta-glucan receptor. Proc Natl Acad Sci U S A. 2007; 104:1366–1370. [PubMed: 17227865]
30. Steele C, Rapaka RR, Metz A, Pop SM, Williams DL, Gordon S, Kolls JK, Brown GD. The beta-glucan receptor dectin-1 recognizes specific morphologies of Aspergillus fumigatus. Plos Pathogens. 2005; 1:e42. [PubMed: 16344862]
31. Hohl TM, Van Epps HL, Rivera A, Morgan LA, Chen PL, Feldmesser M, Pamer EG. Aspergillus fumigatus triggers inflammatory responses by stagespecific beta-glucan display. PLoS Pathog. 2005; 1:e30. [PubMed: 16304610]
32. Saijo S, Ikeda S, Yamabe K, Kakuta S, Ishigame H, Akitsu A, Fujikado N, Kusaka T, Kubo S, Chung SH, Komatsu R, Miura N, Adachi Y, Ohno N, Shibuya K, Yamamoto N, Kawakami K, Yamasaki S, Saito T, Akira S, Iwakura Y. Dectin-2 Recognition of alpha-Mannans and Induction of Th17 Cell Differentiation Is Essential for Host Defense against Candida albicans. Immunity. 2010; 32:681–691. [PubMed: 20493731]
33. Gringhuis SI, Wevers BA, Kaptein TM, van Capel TMM, Theelen B, Boekhout T, de Jong EC, Geijtenbeek TBH. Selective C-Rel Activation via Malt1 Controls Anti-Fungal T-H-17 Immunity by Dectin-1 and Dectin-2. Plos Pathogens. 2011; 7

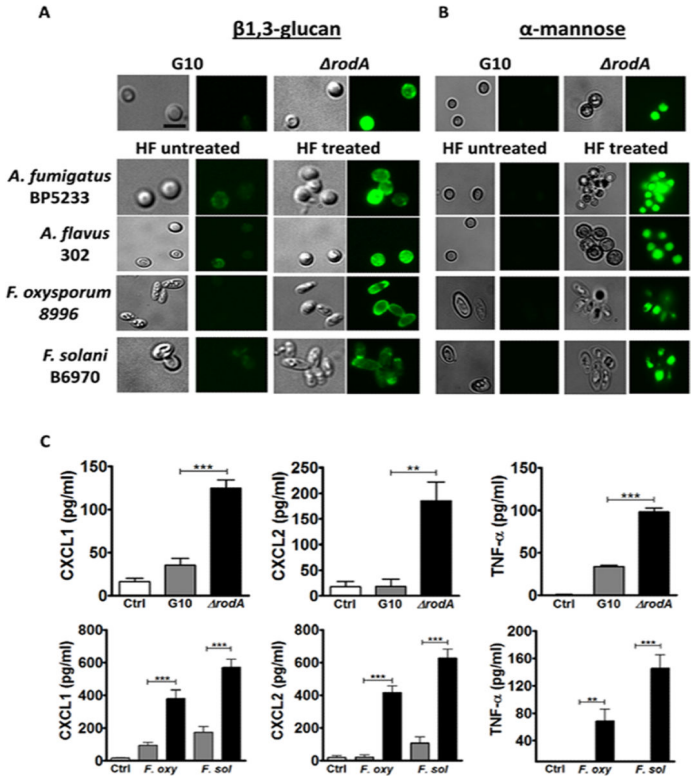

Figure 1. Removal of RodA protein exposes surface β1,3-glucan and α-mannose in *Aspergillus* and *Fusarium* conidia, leading to increased cytokine production by macrophages

A,B) Dormant conidia from *Aspergillus* and *Fusarium* clinical isolates were treated with hydrofluoric acid (HF) to remove the rodlet layer. **A.** HF-treated and Δ*rodA* conidia were fixed with PFA, and β1,3-glucan was detected using a dectin-1-Fc fusion protein and a FITC-conjugated goat anti-mouse IgG secondary antibody. **B.** Concanavalin A (ConA) was used to detect α-mannose, and DyLight 488 Streptavidin was used for detection. Original magnification is x100, and size bar is 2 μm. Cells were visualized by DIC and fluorescent microscopy using oil immersion **C.** C57Bl/6 bone marrow macrophages were incubated 6h with Δ*rodA* or HF treated conidia at a ratio of 1:50 (MOI=50), and CXCL1, CXCL2 and TNF-α secretion was measured by ELISA. These experiments were repeated at least twice with similar results.

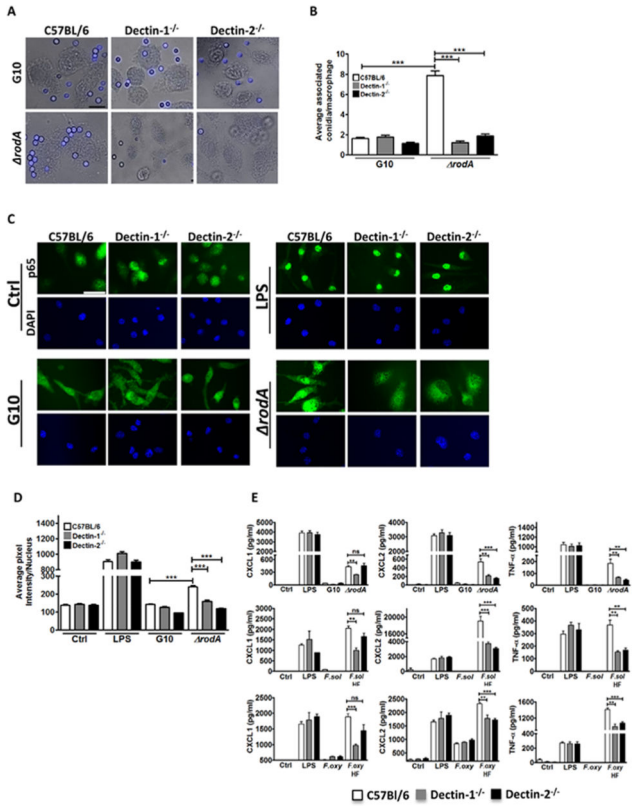

Figure 2. The role of Dectin-1 and Dectin-2 in macrophage activation by Δ*rodA* and HF treated conidia

A. C57Bl/6, Dectin-1$^{-/-}$, and Dectin-2$^{-/-}$ bone marrow macrophages were plated on coverslips and incubated 1h with Δ*rodA* or G10 conidia. Original magnification is x100, and the size bar is 10 μm. **B.** Mean+/-SD associated conidia per macrophage **C.** p65 translocation to the nucleus of C57Bl/6, Dectin-1$^{-/-}$, and Dectin-2$^{-/-}$ bone marrow derived macrophages after 1h incubation with Δ*rodA* conidia. Macrophages were fixed, permeabilized, and stained with anti-p65 primary antibody and Alexafluor-488 tagged anti-rabbit secondary antibody. Cells were visualized by fluorescent microscopy using oil immersion (size bar is 10 μm). **D.** Nuclear translocation was quantified by image analysis using Metamorph software. **E.** CXCL1, CXCL2 and TNF-α production by C57Bl/6, Dectin-1$^{-/-}$, and Dectin-2$^{-/-}$ bone marrow derived macrophages after 6h incubation with Δ*rodA* or HF treated conidia at a ratio of 1:50 (MOI=50). Cytokine production was measured by ELISA. P values are: *<0.05, **<0.001, ***<0.0001. Experiments were performed at least twice with similar results.

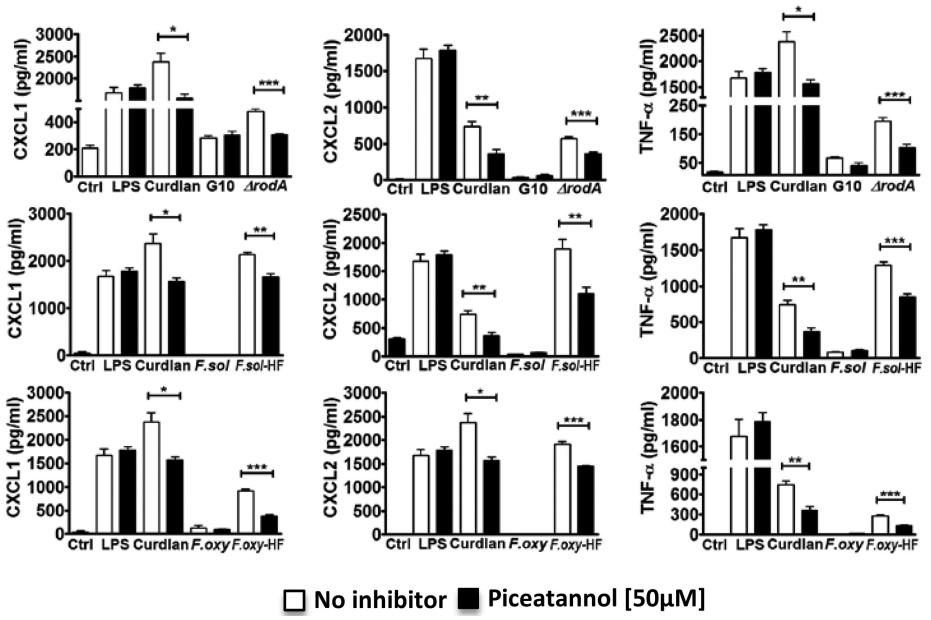

Figure 3. Role of spleen tyrosine kinase (Syk) pathway in macrophage cytokine production

C57Bl/6 macrophages were incubated 6h with Δ*rodA* or HF treated conidia at a ratio of 1:50 (MOI=50) in the presence of a Syk inhibitor (Piceatannol). CXCL1, CXCL2 and TNF-α were measured by ELISA. P values are *<0.05, **<0.001, ***<0.0001. Experiments were performed twice with similar results.

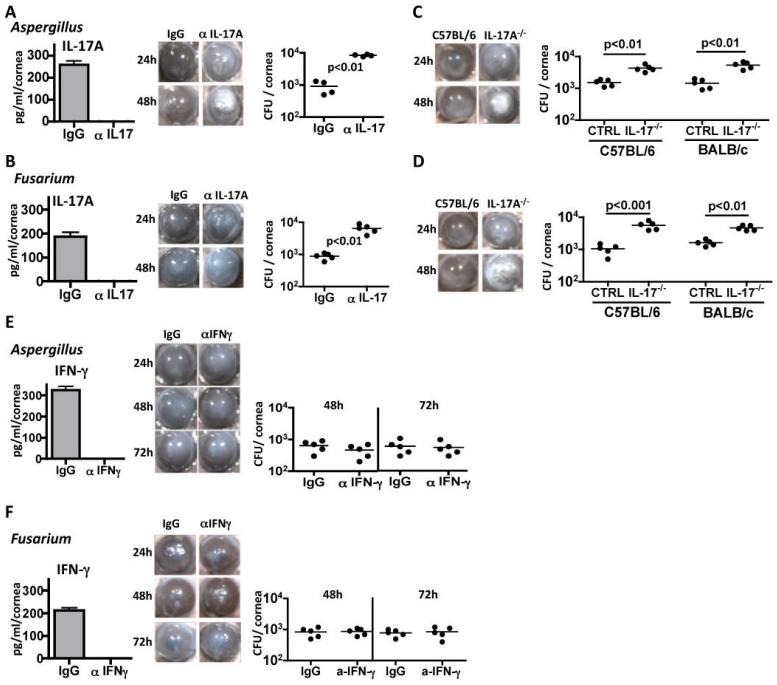

Figure 4. Virulence of *A. fumigatus* Δ*rodA* and G10 strains in infected corneas

5×10^4 live G10 and Δ*rodA* conidia were injected into the corneal stroma of C57Bl/6 mice, and corneal opacity, neutrophil infiltration and CFUs were examined. **A.** Representative corneas at 24h, 48h and 72h post infection with strains G10 or Δ*rodA*, **B, C.** Percent and integrated corneal opacification scores quantified by image analysis (**Figure S2**). **D, E.** Total number of neutrophils and macrophages in the cornea at 24h post infection. Quantification was done by flow cytometry **F.** Colony forming units (CFU) from infected eyes with G10 and Δ*rodA* strains at indicated time points. P value is *<0.05, **<0.001, ***<0.0001. B, C, F: data points represent individual corneas or eyes; D, E: Mean -/-SD of five corneas per group. Experiments were repeated twice with similar results.

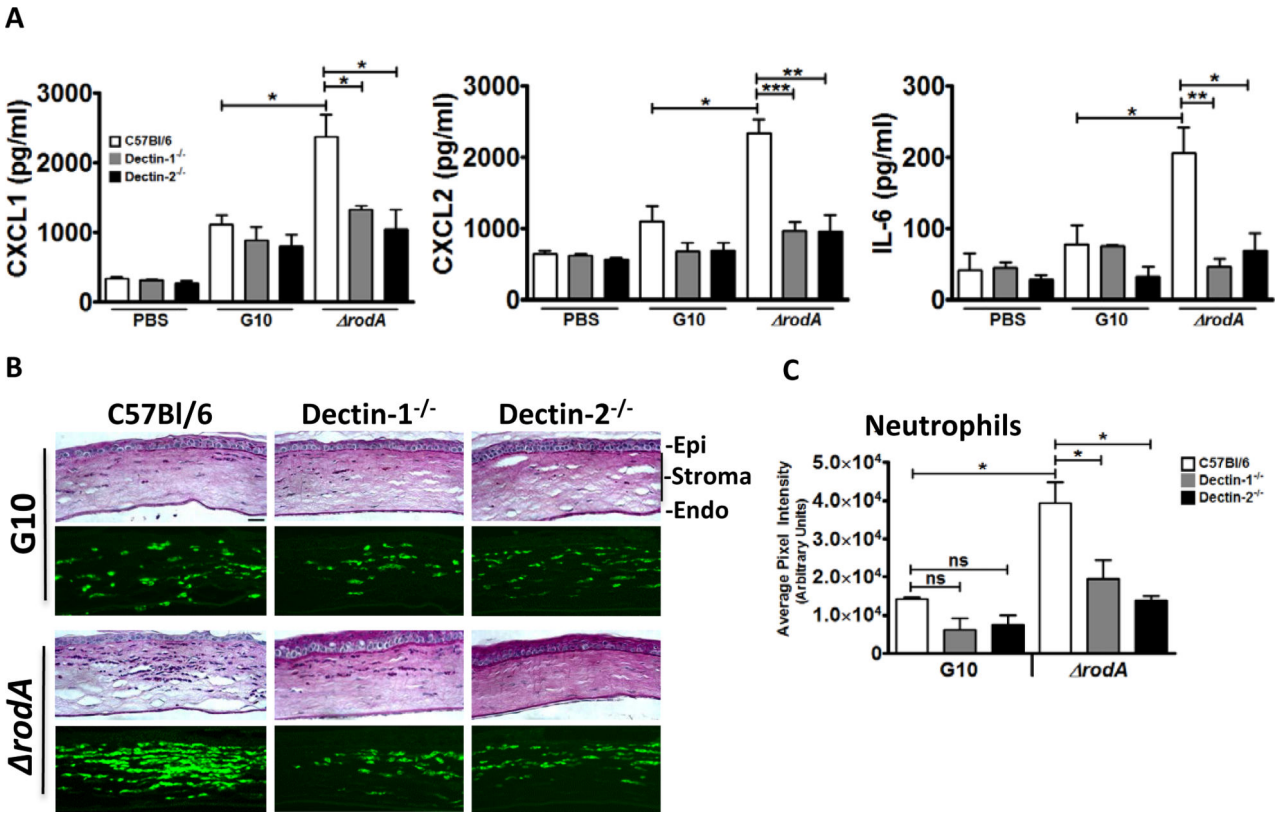

Figure 5. The role of Dectin-1 and Dectin-2 in the early host response following corneal infection with Δ*rodA* and G10 conidia

A. Cytokine production in the cornea at 6h post-infection. C57Bl/6, Dectin-$1^{-/-}$, and Dectin-$2^{-/-}$ mice were injected intrastromally with 5×10^4 G10 or Δ*rodA* conidia as before, and after 6h, corneas were dissected and homogenized, and CXCL1/KC, MIP-2, and IL-6 were measured by ELISA. **B,C.** Histological sections (5 μm) were stained with PASH, or immunostained with NIMP-R14 to detect neutrophils. **B.** Representative sections near the peripheral cornea at the site of neutrophil infiltration. Image bar represents 40X magnification, size bar is 20 μm. **C**. Quantification of NIMPR-14 staining by image analysis (Metamorph) shows average pixel intensity of the entire corneal section (mean+/-SD of five mice per group). P value is *<0.05, **<0.001, ***<0.0001. Experiments were repeated twice with similar results.

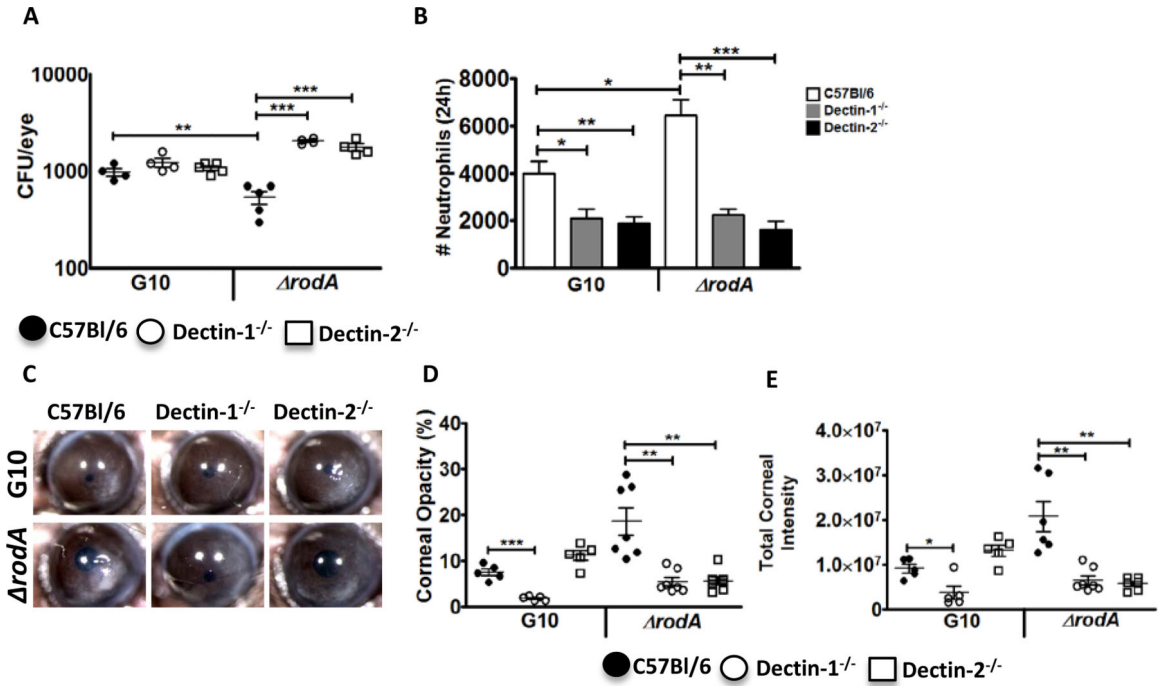

Figure 6. The role of Dectin-1 and Dectin-2 in corneal infection with *A. fumigatus* Δ*rodA*

C57Bl/6, Dectin-1$^{-/-}$, and Dectin-2$^{-/-}$ mice were infected intrastromally with Δ*rodA* or G10 conidia, and CFU, corneal opacity and neutrophil infiltration were assessed after 24h. **A.** CFU in eye homogenate (data points represent individual eyes). **B, C.** Percent and total corneal opacification was quantified by image analysis (data points represent individual eyes). **D.** Representative corneas at 24h post infection. **E.** Total neutrophils in infected corneas. Corneas were dissected and digested with collagenase. Cells were incubated with NIMP-R14 and total neutrophils were quantified by flow cytometry. Data are mean+/-SD of five mice per group. P values are *<0.05, **<0.001, ***<0.0001, and these experiments were repeated twice with similar results.